

Relationship on Oil Cavity Depth and Oil film Flow State of the Large Size Hydrostatic Guide-way

Junpeng Shao ^{1*}, Chunxi Dai ¹, Xiaodong Yang ¹, Yonghai Li ¹, and Zhimin Shi ²

¹ College of Mechanical & Power Engineering, Harbin University of Science and Technology, Harbin150080, China

² Qiqihar CNC Equipment corp, LTD., Qiqihar 161005, China

*Junpeng Shao, yinsi1016@163.com

Abstract

Based on computational fluid dynamics, friction lubrication theory and hydrostatic technology, large size hydrostatic Guide-way of heavy vertical CNC lathes, which are widely used, was taken as research object. The control equation of hydrostatic guide-way's interstitial fluid was established. By finite volume method, lubricating oil properties, boundary conditions such as constant flow inlet, outlet pressure, and wall were set. The velocity distribution of hydrostatic thrust bearing's interstitial fluid was obtained through iterative computations. And influence rules of cavity depth on interstitial oil-film of large size hydrostatic Guide-way's was discussed. The results reflect hydrostatic bearing's internal fluid flow state and provide theoretical basis for the design of practical engineering hydrostatic bearing.

Keywords: flow state, vertical lathe, hydrostatic thrust bearing, finite volume method, interstitial fluid

1. Introduction

Heavy-duty hydrostatic Guide-way plays an important role in the spindle component of lathe, whose property directly affects the machining precision of lathe. The hydrostatic Guide-way utilizes pressure oil-film between rail and rotary table to float bearing spindle and support load. Hydrostatic Guide-way divides into many pads Guide-way and many chambers Guide-way according to whether oil cavity has return chutes or not. The Guide-way which has lateral return chutes between oil cavities is called many pads Guide-way, and which has not a lateral return chute is called many chambers Guide-way. The object of study in this article is many pads Guide-way.

At present many scholars do a certain degree of researches on the oil-film lubrication performance. Singh, Udaya P. took hydrostatic thrust bearing as the research object and built Newton fluid lubricant and non-Newton fluid lubricant, that is the fluid model of lubricating oil mixed into viscosity index improvers or viscosity thickener. He calculated load capacity of two kinds of lubricants by computing the oil cavity pressure distribution under the centrifugal force and comparing the centrifugal inertia effect of two kinds of lubricants [1]. In 2012, Ram, Nathi did a numerical study on micro lubrication problem of hybrid radial bearing. Through reynolds-equation reveals the flows of micro-polar lubricating oil of bearing clearance space, he analyzed lubricating oil micro-polar parameters and the relationship between revolving speed and bearing performance via finite element method and appropriate boundary conditions. The results of numerical simulation indicated the selection of design parameters and micro-polar lubricating oil has a great influence on obtaining the best liquid

oil-film stiffness [2]. Heinrichson Niels and Santos Ilmar Ferreira professor of Technical University of Denmark established the mathematic model about 3-D thermal hydrodynamic lubrication based on Reynolds equation, and researched the capability influence of oil cavity of tilting pad thrust bearings. The result showed that shallow oil cavity has similar characteristic for step bearing, so the shallow oil cavity must affect the capability of bearing [3]. Zhang yan of Harbin Industry Technology carried through numerical simulation about turbine pump hydrostatic bearing using FLUENT software, and discovered the inner flow state of hydrostatic bearing, and analyzed the law that load bearing capability and stiffness capability were affected the parameter of rotating velocity, filler oil pressure, excursion ratio, compensate diameter and oil film thickness, and optimized the structure of bearing [4]. In 2008, Wang Chuangmin numerically solved bearing lubricating film, studied temperature distribution of bearing with dynamic pressure oil film and analyzed the influence of three dimensional temperature field on practical lubrication performance of bearing under given load [5]

Our laboratory applied 3D modeling software Pro/ENGINEER and CFD software FLUENT when researching on hydrostatic guide-way of heavy-duty vertical CNC lathe workbench, comparing velocity distribution and pressure distribution of elliptical cavity with fan-shaped cavity [6-17]. It shows that the velocity fluctuation of elliptical cavity is bigger than fan-shaped cavity's and that the hydrostatic bearing temperature rise is higher than the fan cavity hydrostatic bearing's.

2. Fluid Model of Hydrostatic Guide-way

This essay discusses the constant flux oil supply system of hydrostatic thrust bearing. The feature of it is that every oil pocket of the bearing connects one oil pump of the same flow and the pump sends the transverse flowing lube directly to the oil pocket, forming a pressural lubricant film, buoyantly lifting the main shaft and supporting external load. The working principle is shown in Figure 1.

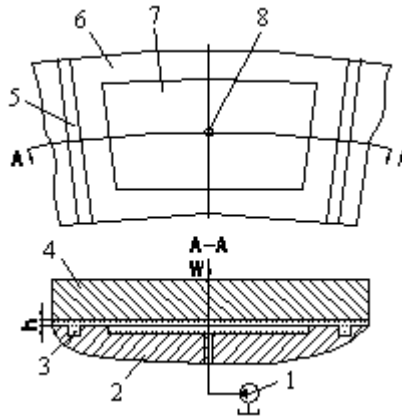


Figure 1. Constant Flux Oil Supply System of Hydrostatic Thrust Bearing 1-pump, 2-guide rail, 3-Interstitial Fluid, 4-rotary Table, 5-return Chute, 6-land, 7-oil Pocket, 8-fuel Feed Hole, w-external Load, h-oil Film Thickness

3. Fluid Model of Hydrostatic Guide-way Clearance

This paper research object that the Interstitial Fluid of hydrostatic guide is cannot compress, and calculation result showed that the Renault coefficient is $Re < 2300$. Because the interior flow of guide is laminar fluid, bring through continuity equation and momentum conservation equation using laminar model.

Continuity equation

$$\frac{\partial \rho}{\partial t} + \nabla \cdot (\rho \mathbf{u}) = 0 \quad (1)$$

The flow is steady state, so the density ρ is not variety with time, $\frac{\partial \rho}{\partial t} = 0$, previous formula can white as:

$$\nabla \cdot (\rho \mathbf{u}) = 0 \quad (2)$$

Also can white as:

$$\nabla \cdot (\rho \mathbf{u}) = \text{div}(\rho \mathbf{u}) = \frac{\partial(\rho u)}{\partial x} + \frac{\partial(\rho v)}{\partial y} + \frac{\partial(\rho w)}{\partial z} = 0 \quad (3)$$

In formula ρ is density, t is time, ∇ is dispersion, u、v、w is the heft of velocity vector u in axle x, y, z directional.

Momentum conservation equation:

$$\frac{\partial(\rho \mathbf{u})}{\partial t} + \text{div}(\rho \mathbf{u}, \mathbf{u}) = \text{div}(\mu \text{grad} \mathbf{u}) - \nabla p + F \quad (4)$$

Above formula decompose three direction equation of axle x, y, z:

$$\begin{aligned} & \frac{\partial(\rho u)}{\partial t} + \frac{\partial(\rho u u)}{\partial x} + \frac{\partial(\rho v u)}{\partial y} + \frac{\partial(\rho w u)}{\partial z} \\ & = \frac{\partial}{\partial x} \left(\mu \frac{\partial u}{\partial x} \right) + \frac{\partial}{\partial y} \left(\mu \frac{\partial u}{\partial y} \right) + \frac{\partial}{\partial z} \left(\mu \frac{\partial u}{\partial z} \right) - \frac{\partial p}{\partial x} + F_x \end{aligned} \quad (4-c)$$

$$\begin{aligned} & \frac{\partial(\rho v)}{\partial t} + \frac{\partial(\rho u v)}{\partial x} + \frac{\partial(\rho v v)}{\partial y} + \frac{\partial(\rho w v)}{\partial z} \\ & = \frac{\partial}{\partial x} \left(\mu \frac{\partial v}{\partial x} \right) + \frac{\partial}{\partial y} \left(\mu \frac{\partial v}{\partial y} \right) + \frac{\partial}{\partial z} \left(\mu \frac{\partial v}{\partial z} \right) - \frac{\partial p}{\partial y} + F_y \end{aligned} \quad (4-b)$$

$$\begin{aligned} & \frac{\partial(\rho w)}{\partial t} + \frac{\partial(\rho u w)}{\partial x} + \frac{\partial(\rho v w)}{\partial y} + \frac{\partial(\rho w w)}{\partial z} \\ & = \frac{\partial}{\partial x} \left(\mu \frac{\partial w}{\partial x} \right) + \frac{\partial}{\partial y} \left(\mu \frac{\partial w}{\partial y} \right) + \frac{\partial}{\partial z} \left(\mu \frac{\partial w}{\partial z} \right) - \frac{\partial p}{\partial z} + F_z \end{aligned} \quad (4-c)$$

In formula p is micro unit pressure of fluid, F_x 、 F_y 、 F_z is the unit power of micro unit, μ is dynamic viscosity of fluid, ρ is density, u、v、w is the heft of velocity vector u in axle

x, y, z directional. ur is heft of velocity, $\text{grad}(\) = \frac{\partial}{\partial x} + \frac{\partial}{\partial y} + \frac{\partial}{\partial z}$.

Based on the above condition, this paper researched the influence of heavy hydrostatic guide fluid state for oil cavity shape. Above equation, F is unit power, hydrostatic thrust bearing just consider the gravitation F_z in the rotary process, so $F_x=F_y=0$, set dynamic viscosity of fluid physical attribute μ equal $0.029 Pa \cdot s$, density ρ equal $880kg/m^3$. Need to note, although energy equation is the basis equation of fluid flow and heat transmission, cannot need to consider the conversation of energy equation in cannot compress flow and not heat exchange.

4. Computed Results and Analysis

To study the influence of the depth of fuel cavity to the velocity field of the hydrostatic guide-way interstitial fluid, simulate the velocity field of interstitial fluid of sectored oil pocket and hydrostatic thrust bearing, with different depth of fuel cavity including 0.25mm, 0.5mm, 1mm, 2mm, 4mm、6mm, 8mm, 10mm and 16mm, under the condition of 17mm return chute's depth, 14mm fuel feed hole's diameter, 0.098kg/s permanent current oil entrance's mass flow-rate, 6r/min and 20r/min rotary tables' angular speed. As shown in figure 2 to figure 13, the result reveals the flowing law of interstitial fluid of sectored oil pocket and hydrostatic thrust bearing. What needs to be stressed out is that the speed unit in the velocity profile is m/s. To avoid lengthiness, the numerical computing result in the condition of 0.5mm and 8mm deep fuel cavity are put below, while that of other conditions can be found in the curve table revealing the relations between the speed of interstitial fluid and the depth of oil cavity.

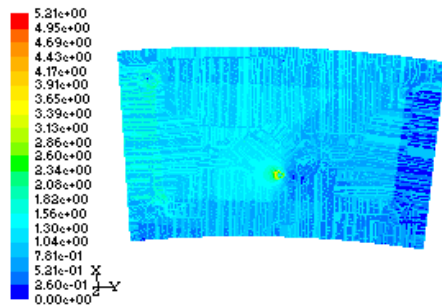


Figure 2. Velocity Field of 0.5mm Deep Cavity

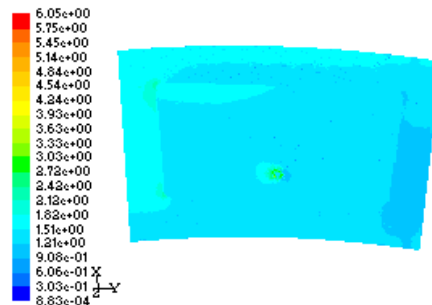


Figure 3. Velocity Vector of 0.5mm Deep Cavity

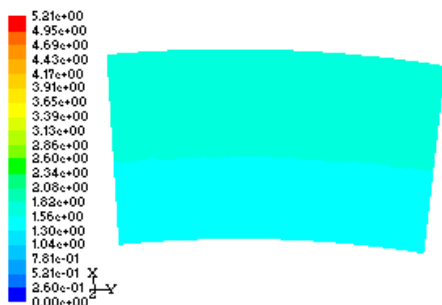


Figure 4. Rotating Wall Velocity of 0.5mm Deep

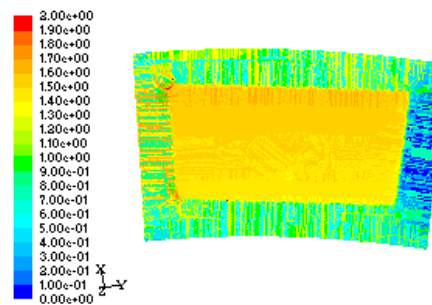


Figure 5. Velocity Field of 8mm Deep Cavity

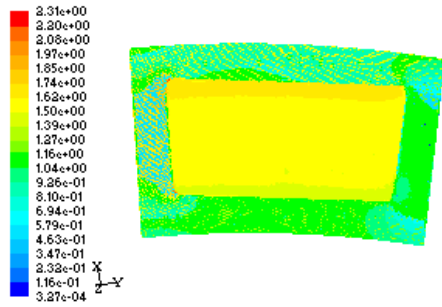


Figure 6. Velocity Vector of 8mm Deep Cavity

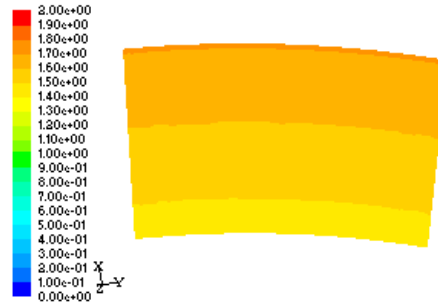


Figure 7. Rotating Wall Velocity of 8mm Deep Cavity

As is shown in the Figure 2 and Figure 5, it illustrates that the velocity distribution rules of hydrostatic guide-way interstitial fluid of 0.5mm and 0.8mm deep cavity are similar when the rotational speed is 6r/min, which conforms to the laws that the speed of sealing oil side from high to low is the left sealing oil side, the radial lateral sealing oil side, the radial inside sealing oil side, the right sealing oil side. But the differences of them are that the velocity distribution of former is more homogeneous than the latter, the oil cavity velocity of the former is almost the same to ambient sealing oil side, and the oil cavity velocity of the latter is obviously higher than ambient sealing oil side. It can be seen from velocity vector Figure 3, Figure 6, that the velocity of lubricating oil is mainly composed of two component velocities: differential pressure velocity and the shear velocity. As can be seen from rotating wall velocity Figure 4, Figure 7, the speed along guide-way from inside to outside gradually increases and reaches the maximum until outer edge, which verifies the conclusion that the linear velocity of fluid contacting with rotating wall is actually proportional to the radius of guide-way.

According to the computed result, we can obtain the influence curve of the oil cavity depth on the maximum velocity when the rotation rates are 6r/min and 20r/min.

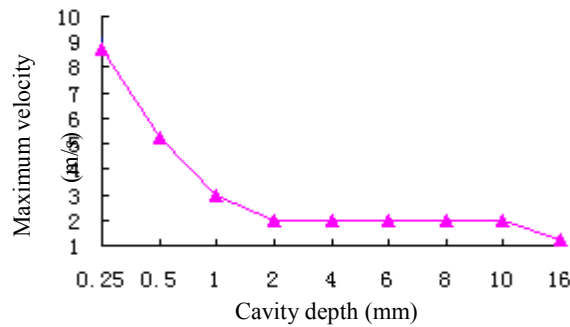


Figure 8. Influence Curve of the Oil on the Maximum Velocity

Figure 8 illustrates that the Maximum speed of the fluid of the large size hydrostatic guide-way clearance increases with the oil cavity depth gradually then decreases then remains unchanged.

5. Conclusion

Hydrostatic guide-way interstitial fluid distribution is obtained by finite volume method. The speed of sealing side from high to low is the lift side, the radial-out side, the inside radial side, the right side.

When the oil cavity area is equivalent, it can be concluded that, the changing rule of velocity on rail of radical is the same by comparing the results of different oil cavity depth. They all increase gradually from the inside to the outside as the oil cavity depth increases. The homogeneity of the velocity distribution is also descending. While the oil cavity depth is the same, the interstitial fluid flow velocity increases as the rotation speed increasing.

Divergence phenomena did not appear during numerical simulation .It indicates that it is stable to solve equation by finite volume method. Meanwhile, the flow distribution of interstitial fluid on hydrostatic guide is accord with the practical. It testifies that the research method is credible.

Acknowledgements

This work was Supported by the National Natural Science Funds for Young Scholar of China (No.51005063, 51075106) and supported by the Heilongjiang Postdoctoral Science-Research Foundation (LBH-Q12062) and Projects of the Special Fund on the Science and Technology Innovation People of Harbin, China (2013RFQXJ086).

References

- [1] P. Udaya Singh, S. Ram Gupta, Kapur and K. Vijay, "On the steady performance of annular hydrostatic thrust bearing", Rabinowitsch fluid model, *Journal of Tribology*, vol. 134, no. 4, (2012), pp. 262-267.
- [2] Ram, Nathi, Sharma and C. Satish, "Analysis of orifice compensated non-recessed hole-entry hybrid journal bearing operating with micropolar lubricants", *Tribology International*, vol. 52, (2012), pp. 132-143.
- [3] N. Heinrichson and S. I. Ferreira, "The influence of injection pockets on the performance of tilting-pad thrust bearings", *Journal of Tribology*, vol. 129, no. 4, (2007), pp. 895-903.
- [4] Z. Yan, "Dynamic Characteristic Analysis and Structure Optimization for the Hydrostatic Bearing of Turbopump", *Journal of Harbin Institute of Technology*, vol. 12, (2007), pp. 17-54.
- [5] W. Chang-min, "Analysis temperature field of hydrostatic bearing based on ANSYS", *Mechanical Management and Development*, vol. 23, (2008), pp. 101-104.
- [6] Y. Xiaodong, "Influence Research of Flow Capacity on Temperature Field of Hydrostatic Thrust Bearing", *Applied Mechanics and Materials*, vol. 427-429, (2013), pp. 225-229.
- [7] Y. Xiaodong, "Simulation on Pressure Field of Gap Oil Film in Constant Flow Hydrostatic Center Frame", *Applied Mechanics and Materials*, vol. 427-429, (2013), pp. 289-292.
- [8] Y. Xiaodong, "Influence Research of Recess Shape on Dynamic Effect of Hydrostatic Thrust Bearing", *Applied Mechanics and Materials*, vol. 274, (2013), pp. 57-70.
- [9] Zhang, Yan-Qin, Fan and Li-Guo, "Simulation and Experimental Analysis on Supporting Characteristics of Multiple Oil Pad Hydrostatic Bearing disk", *Journal of Hydrodynamics*, vol. 25, no. 2, (2013), pp. 236-241.
- [10] Y. Zhang and Y. Qu, "Oil Film Carrying Property Research of Hydrostatic Vertical Guideway of CNC Vertical Lathe", *Key Engineering Materials*, vol. 579-580, (2014), pp. 564-567.
- [11] Y. Xiao-Dong, "Research on Pressure Field of Multi-pad Annular Recess Hydrostatic Thrust Bearing", *Journal of Donghua University (English Edition)*, vol. 30, no. 3, (2013), pp. 254-257.
- [12] Y. Zhang and R. Li, "Research on Hydrostatic Supporting Temperature-Rise of Heavy NC Machine Tool", *Applied Mechanics and Materials*, vol. 274, (2013), pp. 132-135.
- [13] Y. Xiao-Dong, "Numerical Analysis of Flow Field of Circular Cavity Multi-oil-pad Hydrostatic Thrust Bearing with a Sector-shape Cavity", *Journal of Harbin University of Science and Technology*, vol. 18, no. 1, (2013), pp. 41-44.

- [14] Y. Xiao-Dong, "Lubrication Performance and Velocity Characteristics Multi-pad Constant Current Hydrostatic Thrust Bearing", *Journal of Engineering for Thermal Energy and Power*, vol. 28, no. 3, (2013), pp. 296-300.
- [15] Y. Zhang and R. Li, "Temperature Field of Hydrostatic Supporting disk in Different Viscosity and Rotational Speed", *Applied Mechanics and Materials*, vol. 274, (2013), pp. 124-127.
- [16] L. J. Ying and Y. T. Ye, "Study of Electro-Hydraulic Force Servo System Based on Flow Press Servo Valve and Neural Network Intelligent Control Strategy", *Applied Mechanics and Materials*, vol. 427-429, (2013), pp. 1167-1170.
- [17] Z. Yan-qin and C. Yao, "Theoretical Analysis of Bearing Performance of Four Shapes of Recess in Heavy Hydrostatic Bearing", *Journal of Harbin University of Science and Technology*, vol. 18, no. 2, (2013), pp. 68-71.

